Australian Government
Department of Defence
Defence Science and
Technology Group

A Family of Reference Hugoniots for Two-phase Porous Materials

A.D. Resnyansky

Weapons and Combat Systems Division
Defence Science and Technology Group

DST-Group-TR-3152

ABSTRACT

Hugoniot states of heterogeneous materials obtained in shock experiments transit through various thermodynamic states that are not necessarily in equilibrium. Detailed numerical analysis employing a multi-phase constitutive material model has been conducted earlier which stressed the role of achieving equilibrium between the gaseous and condensed phases. The analysis also showed that the abnormal response of highly porous materials is closely associated with the attainment of the inter-phase equilibrium of both pressure and temperature. Mie-Grüneisen equations of state with the Murnaghan cold compression term were used earlier in the numerical analysis to illustrate the abnormal response. The present work shows that very simple equations of state for the phases are sufficient to describe the abnormality with the key necessary consideration a two-phase description of porous materials.

RELEASE LIMITATION

Approved for public release

Published by

Weapons and Counter Measures Division
DSTO Defence Science and Technology Group
PO Box 1500
Edinburgh South Australia 5111 Australia

Telephone: 1300 333 362
Fax: (08) 7389 6567

AR-016-394
June 2015

APPROVED FOR PUBLIC RELEASE

A Family of Reference Hugoniots for Two-phase Porous Materials

Executive Summary

Personnel and platform vulnerability analyses to mitigate effects of Improvised Explosive Devices (IEDs) in the Counter IED and National Security research areas require advanced predictive capabilities. Relevant tools for the analysis are physics based hydrocodes simulating the material response to blast and impact. DSTO (now called DST Group) researchers in cooperation with the TTCP community and universities require adequate material models of advanced materials involved in the mitigation analysis. The main elements specifying any material model are constitutive equations and Equations of State (EOSs). In particular, EOSs for materials representing porous mitigants are frequently obtained from fundamental properties. These properties are determined from first principles by employing material micro-structure and physics of the material response on micro- and meso-level. An important feature of the shock response of highly porous materials is the abnormality manifested as a decrease of the bulk material density as pressure increases. The traditional EOSs do not allow one to describe adequately such material response. To do so, high-temperature non-linear corrections in EOSs are introduced with reference to high-order interactions at the material shock compression. The present work demonstrates that accounting for the inter-phase interaction in the porous material represented as a two-phase mixture is sufficient even if very basic EOSs are employed for the phase materials. The approach allows us to predict features of the material response at high pressures for a wide range of material porosities, and to design reference Hugoniots for porous mitigants, thus, enhancing DSTO modelling capability.

Author

A.D. Resnyansky
Weapons and Combat Systems Division

Anatoly Resnyansky obtained a MSc in Applied Mathematics and Mechanics from Novosibirsk State University (Russia) in 1979. In 1979-1995 he worked in the Lavrentyev Institute of Hydrodynamics (Russian Academy of Science) in the area of constitutive modelling for problems of high-velocity impact. Anatoly obtained a PhD in Physics and Mathematics from the Institute of Hydrodynamics in 1985. He joined the Weapons Effects Group of the Weapons Systems Division (DSTO) in 1998. Anatoly was appointed Adjunct Professor at University of South Australia in 2014. His current research interests include constitutive modelling and material characterisation at high strain rates, ballistic testing and simulation, and theoretical and experimental analysis of multi-phase flows. He has published over one hundred research papers and technical reports.

Contents

This page is intentionally blank

1. Introduction

The shock loading of materials by stimulants such as near-field blast and high-velocity fragment impact requires knowledge of the material response in a wide range of pressures and temperatures. Use of materials containing pores filled with gas (e.g., air) allows experimentalists to increase the temperature range up to extreme values even when loading materials moderately. During such loads porous materials at high porosities may respond in unconventional ways and exhibit abnormalities, which are not captured by conventional equations of state. In order to describe this response, the thermodynamic analyses available in the literature [1-3] focus on incorporation of high-temperature effects into equations of state (EOS) by non-linear additives to conventional EOSs [3]. A Hugoniot is a locus of points connecting the material states in front and behind a shock wave regardless of the thermodynamic path leading to the state behind the front. The Hugoniot analysis extrapolating the response of solid materials to that of porous materials using enhanced EOSs is routinely employed [1, 3]. A comparative analysis has been published elsewhere [2]. An alternative way of building a single-phase EOS [4] is based on a constitutive consideration. The latter approach specifies Hugoniot states from a family of non-equilibrium Hugoniot for a given pressure thus constructing an integral Hugoniot for a porous material. It should be noted that the constitutive single-phase approach [4], or two-phase approaches [5, 6], are physically more sound because they take into account possible non-equilibrium in the state described by a Hugoniot point. However, a simple and universal way of building up Hugoniots when evaluating the mechanical response or constructing EOSs would still be beneficial.

An important feature of using the high temperature adjustments [1-3] when designing an EOS for a porous material is an application of the EOS high-temperature extension to the condensed phase of the porous material. Let us consider two major heat producers during compression of a porous material, which are the adiabatic compression of the gaseous phase and the heat due to plastic work generated from the deformation of particles. The heat due to the plastic work may reach hundreds of degrees in conventional metals [7]. At the same time, temperature due to collapse of pores filled with gas/air may easily exceed thousands of degrees. Therefore, the need to use high-temperature EOS corrections for plastic work is questionable due to the relatively small temperature increase that occurs at the highly localised deformation, regardless of the deformation nature. Some of the heating mechanisms mentioned in the literature [7] are cracking, adiabatic shear banding, cumulative jetting, etc. In addition, the flow from the gaseous phase to the condensed phase could be much higher but it does take some time. Heat transfer from the collapsing gaseous phase to the condensed phase also depends on the size of particles and the heat conductivity of the condensed phase. The heat transfer may take from a few nanoseconds up to fractions of microseconds and even a few microseconds [5]. Therefore, for some shocked porous materials the heat absorbed by the condensed phase may be relatively slow and use of the high-temperature EOS corrections in the condensed phase may be unnecessary. At the same time, the abnormality, for treatment of which the EOS corrections are introduced, is observed in practically any porous material provided that porosity is sufficiently high. Thus, an extra influential factor could be missed which could

explain why the abnormality occurs for the porous material as a whole rather than just for the condensed phase.

When conducting the constitutive numerical analysis [5, 6] of two-phase porous materials employing conventional Mie-Grüneisen equations of state, previous studies have demonstrated the importance of a two-phase description of abnormalities at high material porosities. The analysis indicated that the time required for the inter-phase equilibrium between certain variables in shock wave compression is critical. For example, the shock waves resulting in extreme pressures may not provide sufficient time to achieve temperature equilibrium between the phases, whereas at moderate shock pressures below a threshold pressure the equilibrium might be achieved. The analysis employed a simplified version of EOS [8] with the Murnaghan cold compression term [9, 10] demonstrated [5] that the abnormality is typically manifested for a highly porous material when pressure and temperature equilibrium between the phases has been achieved. Remarkably, the conventional behaviour of the Hugoniot is observed if phase temperatures are not in equilibrium and this occurs at higher pressures because the corresponding shock wave provides a faster transition than when equilibrium is obtained. The non-linear form of this EOS allowed the author [5] to analyse the abnormality only numerically for the case when different equilibriums between the phases, namely, non-equilibrium (independent thermodynamic states), pressure, and pressure-temperature equilibriums were assumed. Another less likely equilibrium assumption such as the sole temperature equilibrium has been analysed for a two-phase solid material subject to phase transitions [11]. In the analyses [5, 6] it has been shown that the abnormality for highly porous materials is typical in the case of both pressure and temperature equilibriums between the phases.

We show here that the choice of an equation of state for the phases is not critical, but the two-phase consideration might be used to detect an abnormality of the Hugoniot. In order to analyse the Hugoniot behaviour, the present work employs simplest EOSs thermodynamically consistent with shock-wave compression. For the gaseous phase, the simplest EOS consistent with shock compressibility and heating is the ideal gas EOS, and for the condensed phase, a similar EOS is a stiffened EOS. The important feature of an EOS is selection of a constant power exponent for the polytropic gas, and constant positive Grüneisen parameters for the stiffened EOS. It will be shown that in the case of pressure and temperature equilibrium between the phases of a highly porous material the abnormal behaviour is typical, and the conditions of abnormality will be derived for these EOSs. The present analysis will deal with the typical types of parameter equilibrium observed within the shock wave propagation that includes two scenarios, namely, the pressure and temperature equilibrium resulting in possible Hugoniot abnormality, and in pressure equilibrium and temperature non-equilibrium in the case of faster compression at the shock loading above the threshold pressure.

The present work demonstrates that selection of the two-phase consideration with such simple EOSs enables us to derive an analytical EOS for the porous material. The resulting composite EOS is shown to be sufficient for description of the abnormality and the main important high-pressure features of the material response. During the analysis, it is

observed that the Grüneisen parameter is the key one controlling the Hugoniot behaviour at high pressures.

2. Hugoniot with the Pressure-temperature Equilibrium

The Rankine-Hugoniots conditions derived from the mass, momentum and energy conservation laws across the shock jump routinely include the following equations [1]:

$$\rho(D-u)=\rho_f D\,,\quad p-p_f=\rho_f D u$$
$$e-e_f=\tfrac{1}{2}(p+p_f)\left(\frac{1}{\rho_f}-\frac{1}{\rho}\right) \qquad (1)$$

here the parameters are associated with the laboratory system where the material is stationary in front of the shock wave. The states in front of the wave are referred by the subscript '*f* ', D is the shock velocity, e is specific internal energy, ρ is material density related to specific volume v as $v = 1/\rho$, p is pressure and u is particle velocity.

For a material fully specified by two independent thermodynamic parameters such as pressure and specific volume, the last equation of (1), a consequence of the energy conservation law from the three conservation laws, is sufficient to determine the Hugoniot as $p = p_H(v)$ if an EOS in the form $e = e(p,v)$ is given. This approach, as discussed in the previous section, is routinely used for analysis of condensed materials and frequently extrapolated to the porous material case.

The first part of the present analysis will deal with the states loaded to pressure below the pressure threshold and, therefore, the equilibrium of pressure and temperature between the phases is assumed.

It should be mentioned that even with common pressure and temperature parameters in the case of the equilibrium, specific volume is an individual characteristic of each phase. At the same time, for the Hugoniot determination, when compressing a porous material with a flyer plate or with the use of explosive products, providing a given pressure p or velocity u behind the shock front, we need to identify individual characteristics. These are specific volumes v_1 and v_2 or densities ρ_1 and ρ_2 ($v_k = 1/\rho_k$, $k = 1,2$), for condensed and gaseous phases, respectively, from independent EOSs for the phases. Due to its two-phase nature, the additivity rule has to be applied to internal energy and specific volume:

$$e = c_1 e_1 + c_2 e_2$$
$$v = c_1 v_1 + c_2 v_2 \qquad (2)$$

here c_1 and c_2 are mass concentration of the condensed and gaseous phases respectively such that $c_1 + c_2 = 1$. Therefore, the actual change of specific volumes depends on individual capacity of each phase to be compressed, and the thermal characteristics are

affected by individual thermo-physical laws for each of the phases dictated by individual EOSs. The above-mentioned Mie-Grüneisen-type simple EOSs specified for each of the phases are:

$$e_1 = \frac{p_1 + \gamma_1 p_0}{\gamma_{1m}\rho_1}$$
$$e_2 = \frac{p_2}{\gamma_{2m}\rho_2} \qquad (3)$$

Here $\gamma_{km} = \gamma_k - 1$, γ_{km} (k = 1,2) are the Grüneisen parameters (γ_2 is the polytropic index for the gaseous component), p_0 is the stiffening constant for the condensed material EOS, $p_0 = \rho_{10}c_{10}^2/\gamma_1$. Denotation $\Gamma = \gamma_{1m}$ for the Grüneisen parameters in the solid constituent will also be used below. The arbitrary parameters e_{k0} are the calibrating constants which could be formally selected, for example, to adjust the internal energies to constants, e_{0k}, at the normal conditions at $p = p_a$ and $\rho_k = \rho_{k0}$ (k = 1, 2) with the reference densities ρ_{k0} so that $e_{10} = (p_a + \gamma_1 p_0)/(\gamma_{1m}\rho_{10})$ and $e_{20} = p_a/(\gamma_{2m}\rho_{20})$.

Constant heat capacities c_{v1} and c_{v2} are assumed for each phase where $c_v = (\partial e/\partial T)_v$. Then the EOSs (3) allow one to determine temperatures for each of the phases:

$$T_1 = \frac{1}{c_{v1}}\frac{p_1 + p_0}{\gamma_{1m}\rho_1}$$
$$T_2 = \frac{1}{c_{v2}}\frac{p_2}{\gamma_{2m}\rho_2} \qquad (4)$$

The equations above, which are specific for each of the phases of the two-phase mixture, are to be completed by the equilibrium conditions following the present assumptions:

$$p = p_1$$
$$p_1 = p_2 \qquad (5)$$
$$T_1 = T_2$$

Summarising, we have the system of 10 equations, including one energy conservation law across the shock jump in Equation (1), two additivity rules expressed by Equation (2), four formulations of the phases' equations of state (Equations (3) and (4)), and three equilibrium conditions formulated in Equation (5). This system contains 11 independent variables, namely, e, p, v, e_1, e_2, p_1, p_2, v_1, v_2, T_1, and T_2. It should be noted that for the single-phase material there is no need in the auxiliary formulation (Equation (4)) of EOSs for temperature because the temperature limitations are not imposed on a single-phase material.

Thus, similarly to the conventional single-phase case we have a thermodynamical parameter, for example, pressure p, which we should be able to use to determine the remaining parameters, including all parameters of the individual phases. In the next

section we will specify the Hugoniot in an explicit form and analyse when the abnormality may occur.

3. Analysis of the Hugoniot Abnormality

In this section we derive an Hugoniot on the assumption of thermal and force equilibrium. We assume that the state 'f' is associated with the reference state in the laboratory system selected such that $u_f = 0$, which has the reference specific volume for the mixture $v_f = c_1 v_{01} + c_2 v_{02}$, where $v_{01} = 1/\rho_{01}$ and $v_{02} = 1/\rho_{02}$; ρ_{01} and ρ_{02} are the reference densities of the individual condensed and gaseous phases. The 'f'-state is associated with $p_f = p_a$ and $e_f = 0$, where p_a is ambient pressure.

The energy conservation law in Equation (1) with substitutions from EOSs (Equations (3)) gives:

$$c_1(p+\gamma_1 p_0)v_1/\gamma_{1m} + c_2 p v_2/\gamma_{2m} - e_0 = \tfrac{1}{2}(p+p_f)(v_f - v) \tag{6}$$

where the following denotation is used $e_0 = c_1 e_{01} + c_2 e_{02}$.

The additivity rule (Equation (2)) for the specific volume and the temperature equilibrium conditions (5) along with necessary EOSs (4) give another two equations:

$$\begin{aligned} &v = c_1 v_1 + c_2 v_2 \,, \\ &\frac{(p+p_0)v_1}{c_{v1}\gamma_{1m}} = \frac{p v_2}{c_{v2}\gamma_{2m}} \,. \end{aligned} \tag{7}$$

Thus, the reduced system of three Equations (6) and (7) for four parameters p, v_1, v_2, and v allows us to derive the Hugoniot $p = p_H(v)$. Specifically, we can express v_1 and v_2 from (7) as dependencies on p and v and after substitution in (6) we have Hugoniot in the following form:

$$\frac{c_1 c_{v1}(p+\gamma_1 p_0) + c_2 c_{v2}(p+p_0)}{c_1 c_{v1}\gamma_{1m} p + c_2 c_{v2}\gamma_{2m}(p+p_0)} \times pv - e_0 = \tfrac{1}{2}(p+p_f)(v_f - v). \tag{8}$$

Denoting $c'_{v1} = c_1 c_{v1}$ and $c'_{v2} = c_2 c_{v2}$ and introducing the denotations below for the thermo-mechanical characteristics of the mixture:

$$\begin{aligned} &c_{vs} = c'_{v1} + c'_{v2} \,, \quad c_{vg} = c'_{v1}\gamma_1 + c'_{v2} \\ &c_{vm} = c'_{v1}\gamma_{1m} + c'_{v2}\gamma_{2m} \,, \quad c_{v2m} = c'_{v2}\gamma_{2m} \end{aligned}$$

we can rewrite (8) in the following compact form:

$$p(c_{vs} p + c_{vg} p_0)v - e_0(c_{vm} p + c_{v2m} p_0) = \tfrac{1}{2}(p+p_f)(v_f - v)(c_{vm} p + c_{v2m} p_0) \tag{9}$$

The Hugoniot $p = p_H(v)$ can be found by solution of the quadratic Equation (9). The analysis shows that for a positive discriminant of Equation (9), two different pressure values corresponding to the same specific volume exist as a solution of the equation. These pressures have physical meaning and they indicate the Hugoniot abnormality. For the sake of convenience, we can conduct an analysis of the inversed Hugoniot $v = v_H(p)$ that is free of the multifold issue.

Equation (9) in the inverse form can be written as follows:

$$v = \frac{\left[\frac{1}{2}\left(p + p_f\right)v_f + e_0\right]\left(c_{vm}\,p + c_{v2m}\,p_0\right)}{p\left(c_{vs}\,p + c_{vg}\,p_0\right) + \frac{1}{2}\left(p + p_f\right)\left(c_{vm}\,p + c_{v2m}\,p_0\right)}. \tag{10}$$

The abnormality occurs for particular thermo-mechanical material constants and a combination of pressure and specific volume. For a conventional Hugoniot represented as $p = p_H(v)$ or $v = v_H(p)$, this event, expressed by the relation $(\partial v_H/\partial p) > 0$, cannot occur due to thermodynamical limitations for the corresponding EOS. In the present case, when pressure and specific volume are not linked via a single EOS, this is possible.

In order to formulate the abnormality condition in a compact representation, we can consider an approximation of Equation (10) at $p_f = 0$:

$$v = \frac{\left(\frac{1}{2}\,pv_f + e_0\right)\left(c_{vm}\,p + c_{v2m}\,p_0\right)}{p\left(c_{vsm}\,p + c_{vgm}\,p_0\right)} \tag{11}$$

where

$$c_{vsm} = c_{vs} + \tfrac{1}{2}c_{vm}\,, \quad c_{vgm} = c_{vg} + \tfrac{1}{2}c_{v2m}$$

In order to substantiate the use of Equation (11), we evaluate difference δ between the solution of Equations (10), $v(p, \varepsilon)$, and (11), $v(p, 0)$, using $p_f = \varepsilon$ as a small parameter. A first order approximation of the difference is:

$$\delta = v(p,\varepsilon) - v(p,0) \approx v(p,0) + v_\varepsilon(p,0)\varepsilon - v(p,0) = v_\varepsilon(p,0)\varepsilon$$

This equation is applicable because the solution (Equation (10)) at $\varepsilon = 0$ is identical to the solution (Equation (11)), as easily checked. The derivative of $v(p, \varepsilon)$ over ε calculated from Equation (10) at $\varepsilon = 0$ is obviously finite because the denominators in Equations (10) and (11) are positive for finite v. Thus, the solution (Equation (11)) is a sufficient approximation, if the loading pressure is orders higher than the atmospheric one. This is the case for the shock loading of porous materials when the shock pressure exceeds the ambient pressure by several orders of magnitude. If necessary, in case of weak shocks, Equation (10) can be analysed directly.

If we consider the analysis of the solution (Equation (11)), we can calculate derivative $\partial v_H/\partial p$ at any given p as follows:

$$\frac{\partial v}{\partial p} = \left\{\left[\tfrac{1}{2} v_f \left(c_{vm} p + c_{v2m} p_0\right) + \left(\tfrac{1}{2} p v_f + e_0\right) c_{vm}\right] p \left(c_{vsm} p + c_{vgm} p_0\right) - \right.$$
$$\left. - \left(\tfrac{1}{2} p v_f + e_0\right)\left(c_{vm} p + c_{v2m} p_0\right)\left(2c_{vsm} p + c_{vgm} p_0\right)\right\} \Big/ \left[p\left(c_{vsm} p + c_{vgm} p_0\right)\right]^2 \qquad (12)$$

The sign of the derivative (12) is coincident with that of the numerator. The numerator can be rewritten as follows:

$$\begin{aligned} & ap^2 - 2bp - c \\ & a = \tfrac{1}{2} p_0 v_f \left(c_{vg} c_{vm} - c_{v2m} c_{vs}\right) - e_0 c_{vm} \left(c_{vs} + \tfrac{1}{2} c_{vm}\right) \\ & b = e_0 c_{v2m} \left(c_{vs} + \tfrac{1}{2} c_{vm}\right) p_0 \\ & c = e_0 c_{v2m} \left(c_{vg} + \tfrac{1}{2} c_{v2m}\right) p_0^2 \end{aligned} \qquad (13)$$

Discriminant $D_0 = b^2 + ac$ of the numerator (13) (scaled by $1/(e_0 p_0)$) is:

$$D_0 = \left[c_{v2m}\left(c_{vs} + \tfrac{1}{2} c_{vm}\right)\right]^2 + \left[\frac{1}{2}\frac{p_0 v_f}{e_0}\left(c_{vg} c_{vm} - c_{v2m} c_{vs}\right) - c_{vm}\left(c_{vs} + \tfrac{1}{2} c_{vm}\right)\right] c_{v2m}\left(c_{vg} + \tfrac{1}{2} c_{v2m}\right). \qquad (14)$$

The numerator (the first row in system (13)) has initially (at small p) a negative sign due to $c < 0$ that does not change if the denominator is negative. Otherwise, when the pressure increases, the denominator sign changes at the following critical pressure p_c:

$$p_c = \frac{\sqrt{D_0} - c_{v2m}\left(c_{vs} + \tfrac{1}{2} c_{vm}\right)}{\frac{1}{2}\frac{p_0 v_f}{e_0}\left(c_{vg} c_{vm} - c_{v2m} c_{vs}\right) - c_{vm}\left(c_{vs} + \tfrac{1}{2} c_{vm}\right)} p_0 \qquad (15)$$

We define a critical initial specific volume v_b as a limit of volumes v_f, above which the abnormality takes place for the Hugoniots with $v_f > v_b$. This volume can be easy found from Equation (14) when D_0 is changing its sign to positive at $D_0 = 0$, which gives

$$v_b = \frac{2e_0}{p_0}\left(c_{vs} + \tfrac{1}{2} c_{vm}\right) \frac{\dfrac{c_{v2m}\left(c_{vs} + \tfrac{1}{2} c_{vm}\right)}{c_{vg} + \tfrac{1}{2} c_{v2m}} + c_{vm}}{c_{vg} c_{vm} - c_{v2m} c_{vs}}. \qquad (16)$$

The case resulting in the Pressure-Temperature Equilibrium (PTE) Hugoniot $v_H^{PTE}(p)$, has been fully analysed above, following established terminology [5].

Commenting on the specific volume v_b, if pressure and temperature were in equilibrium for the whole process of the shock loading and $v_f > v_b$, which means that the Hugoniot is abnormal, then it would be easy to show that $v > v_b$ for any point of the given PTE Hugoniot and v_b would be a lower limit of specific volume. Thus, in the case of abnormal Hugoniot v_b also plays the role of limiting volume. If there was a transition to another regime with pressure equilibrium and temperature non-equilibrium v_b may be not the limiting volume in a global sense and the actual limiting volume may be managed by the alternative Hugoniot. This case will be analysed in the next section.

4. The Pressure Equilibrium and Composite Hugoniots

Following the established analysis [5], another limiting case for possible Hugoniot states relates to the Pressure Equilibrium (PE) and independent temperatures in the phases. For this case with the resulting PE Hugoniot $v_H^{PE}(p)$, each phase is subject to independent shock compression identified by the same final pressure behind the shock front [5]. For the case of ambient pressure in front of the wave, $p_f = p_a$, application of the jump conditions to the individual phases with EOSs (Equations (3)) gives the following well-known Hugoniots for the condensed and gaseous phases:

$$\begin{aligned} v_1 &= v_{01}\frac{(p_f + p_0)\gamma_{1p} + (p_1 + p_0)\gamma_{1m}}{(p_1 + p_0)\gamma_{1p} + (p_f + p_0)\gamma_{1m}} \\ v_2 &= v_{02}\frac{p_f\gamma_{2p} + p_2\gamma_{2m}}{p_2\gamma_{2p} + p_f\gamma_{2m}} \end{aligned} \tag{17}$$

where $\gamma_{kp} = \gamma_k + 1$ (k = 1,2).

The Equations (17) along with the equilibrium conditions for pressure and the additivity rule (Equation (2)) for the specific volume form the following system:

$$\begin{aligned} v &= c_1 v_1 + c_2 v_2 \\ p_1 &= p_2 \\ p_1 &= p \end{aligned} \tag{18}$$

Thus, for 6 variables p, v, p_1, p_2, v_1, and v_2 we have 5 equations (Equations (17)-(18)) which can be easily reduced to the following Hugoniot for the two-phase mixture:

$$v = c_1 v_{01}\frac{(p_f + p_0)\gamma_{1p} + (p + p_0)\gamma_{1m}}{(p + p_0)\gamma_{1p} + (p_f + p_0)\gamma_{1m}} + c_2 v_{02}\frac{p_f\gamma_{2p} + p\gamma_{2m}}{p\gamma_{2p} + p_f\gamma_{2m}}. \tag{19}$$

The derivative $\partial v/\partial p$ for this Hugoniot can be directly calculated from Equation (19) and the result is:

$$\frac{\partial v}{\partial p} = -\frac{4\gamma_{1m}c_1 v_{01}}{\left[(p+p_0)\gamma_{1p} + (p_f + p_0)\gamma_{1m}\right]^2} - \frac{4\gamma_{2m}c_2 v_{02}}{\left[p\gamma_{2p} + p_f\gamma_{2m}\right]^2}. \quad (20)$$

The relation (Equation (20)) clearly demonstrates that this Hugoniot has no abnormality due to $\partial v/\partial p < 0$ for any pressure. Similar to the case of conventional single-phase Hugoniots based on a Mie-Grüneisen EOS, when pressure increases infinitely, the limiting specific volume v_a (the subscript 'a' refers to the Hugoniot associated with the one eventuated above the pressure threshold) for the PE Hugoniot can be easily found from Equation (19) as follows

$$v_a = c_1 v_{01}\frac{\gamma_{1m}}{\gamma_{1p}} + c_2 v_{02}\frac{\gamma_{2m}}{\gamma_{2p}}$$

It should be kept in mind however that the actual limiting specific volume may differ from this value and be controlled by the PTE Hugoniot if $v_b < v_a$.

We can assume that with increasing strength of shock wave and, thus, pressure behind the shock, the shock front width is decreasing along with the time of inter-phase equilibrating of thermodynamical parameters [5]. Hypothetically, the time of transformation in the shock wave can be so short in the material such that even pressure equilibrium is not achieved, which can be described by a Non-Equilibrium Hugoniot [5]. Alternatively, in some exotic imaginable cases the temperature equilibrium occurs prior the pressure equilibrium, the Hugoniot may be better described by a Temperature Equilibrium Hugoniot [11]. However, such cases are physically less likely than the case of Pressure Equilibrium (PE) and Pressure-Temperature Equilibrium (PTE) analysed above.

Thus, accepting the transition from the pressure and temperature equilibrium to solely the pressure equilibrium with the final pressure increasing behind the shock front, we have the PTE and PE cases predominantly. Numerical analysis of the inter-phase equilibrium for both pressure and temperature associated with the Hugoniot state obtained in experiment is likely to be achieved at pressures up to a pressure threshold that may be taken as a point of intersection between the PTE and PE Hugoniots [5]. An alternative scenario is the wave specified by the behind-shock final pressure that is above the threshold pressure. In this case, the transition within the shock front may occur during such a short time that the thermal equilibrium has not been achieved leaving the material at the pressure equilibrium only. The pressure equilibrium occurs well before the main shock front within a pre-compaction precursor wave [5]. A combination of the PTE Hugoniot below the threshold and the PE Hugoniot above the threshold gives us a single composite Hugoniot denoted below by $v_H{}^S(p)$.

An example beyond the single composite Hugoniot case would be a porous material with large solid particles surrounded by significant gaseous pockets, which may prevent achieving temperature equilibrium even at the slow rate of loading occurring at a final pressure below the threshold. This may result in an extension of the PE Hugoniot contribution, $v_H{}^{PE}(p)$, into $v_H{}^S(p)$ below the threshold. On the other side, a porous material with ultra-dispersed particles within the nanometer size region may lead to achieving pressure-temperature equilibrium even for very quick loading corresponding to a large

final pressure, thus resulting in an extension of the PTE Hugoniot contribution, $v_H^{PTE}(p)$, into $v_H^S(p)$ above the threshold pressure. Some of the extensions occurring for real materials will be illustrated below on the case-to-case basis.

The case accepted for derivation of an analytical EOS is the composite Hugoniot obtained with the above-described rule. Due to possible multi-valuedness of the PTE Hugoniot, the Hugoniot will be represented as specific volume versus pressure. It should be noted that this form is acceptable for the present EOSs (Equations (3)-(4)). However this presentation may be cumbersome for EOSs where multi-valuedness is possible for the thermodynamic variable of specific volume if, for example, the Van-der-Waals EOS is used for one of the phases.

Summarising, the combined single Hugoniot can be represented in the following simple form from the contributing Hugoniots

$$v_H^S(p) = \min\left\{v_H^{PTE}(p), v_H^{PE}(p)\right\}. \tag{21}$$

It should be noted that the transition from the PTE Hugoniot, $v_H^{PTE}(p)$, to the PE Hugoniot, $v_H^{PE}(p)$, at the threshold pressure occurs not only for the abnormal PTE Hugoniot within the experimentally observed pressure range. Illustrations in the next section will demonstrate when this is the case for the PTE Hugoniots with conventional behaviour.

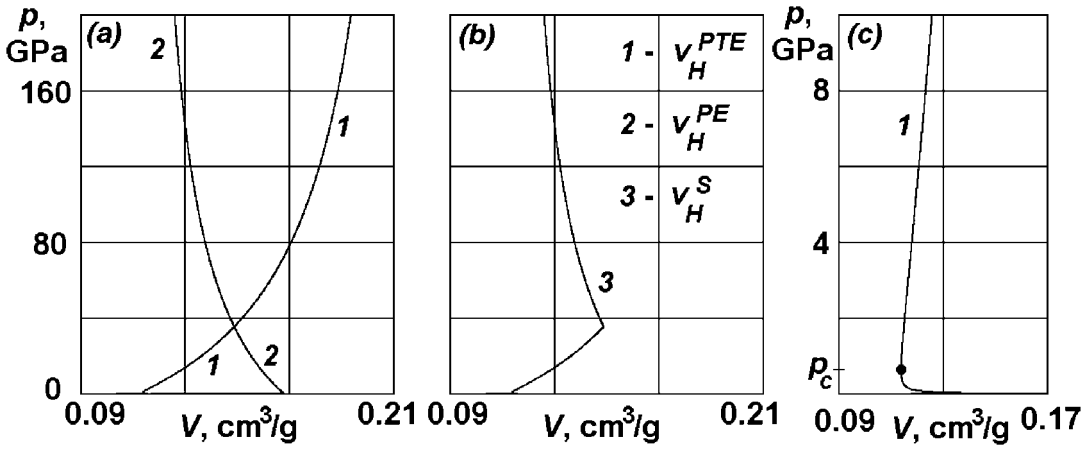

Figure 1 Schematic of derivation of the Hugoniot $v_H^S(p)$ from the pressure-temperature equilibrium Hugoniot $v_H^{PTE}(p)$ and the pressure equilibrium Hugoniot $v_H^{PE}(p)$.

The algorithm of construction of the composite Hugoniot $v_H^S(p)$ is illustrated in Fig. 1. Thermo-mechanical constants used for the contributing Hugoniots, $v_H^{PTE}(p)$ from Equation (10) and $v_H^{PE}(p)$ from Equation (19), will be specified in details in the subsequent section. Copper powder is used to illustrate the use of the Hugoniots, using a porosity m = 4, where $m = \rho_{01}/\rho_0$, and ρ_0 is the average density of the powder tested. As seen in Fig. 1 (a) with the legend in Fig. 1(b), curve 1 (the Hugoniot $v_H^{PTE}(p)$) intersects curve 2 (the Hugoniot $v_H^{PE}(p)$). The composite Hugoniot $v_H^S(p)$ (curve 3 in Fig. 1(b)) is combined from sections of the contributing Hugoniots with the specific volume taking the minimal value

as follows from the representation in Equation (21). It may seem that the abnormal Hugoniot (curve 1 in Fig. 1(a)) has no critical point defined by equation (15) when the Hugoniot $v_H^{PTE}(p)$ changes its slope. However, both curves 1 and 2 must originate from the same point $v = v_f$ at atmospheric pressure. When analysing closely the corresponding fragment of curve 1 in Fig. 1(a), the result can be seen in Fig. 1(c) with easily identifiable critical pressure p_c.

The next section will illustrate how the Hugoniot $v_H^S(p)$ calculated from Equation (21), when composing the pressure-temperature branch $v_H^{PTE}(p)$ from Equation (10) and the pressure branch $v_H^{PE}(p)$ Equation (19), agrees with available experimental observations, and what limitations the derived Hugoniot might have.

5. Numerical Examples

The analytical Hugoniot for porous material will be illustrated below with a number of calculated Hugoniots compared with experiments for several metallic powders, an organic porous material and a porous rock composition in a wide variety of porosities. All the examples will be calculated with the reference pressure equal to atmospheric p_a = 0.1 MPa. For the air at room temperature T = 300 K, only two constants are needed in order to specify EOS represented by the second equations from the pairs (3)-(4). To represent the air we select well tabulated values c_{02} = 0.34 km/s and γ_2 = 1.4. For a solid constituent we need four constants to specify the corresponding EOS, which can be accomplished by specifying ρ_{01}, c_{01}, c_{v1}, and Γ.

Table 1 Equation of State constants employed for solid constituents of porous materials and the calculated limiting density corresponding to the abnormality transition.

	ρ_{01}, g/cm^3	c_{01}, km/s	c_{v1}, J/(g·K)	Γ	ρ_b, g/cm^3	m_b
Cobalt	8.82	4.79	0.4145	1.99	4.4	2.0
Copper	8.93	3.94	0.45	1.97	4.43	2.02
Iron	7.84	4.6336	0.45	2.2	4.1	1.91
Molybdenum	10.2	5.42	0.256	1.61	5.06	2.02
Zinc	7.14	4.6	0.39	1.6	3.17	2.25
Calcite	2.71	5.08	1.2	1.18	0.58	4.6
PMMA	1.186	2.32	1.6	0.5	0.24	4.94

As examples of condensed constituent for the metallic powders we take Cobalt, Copper, Iron, Molybdenum and Zinc. We take calcite ($CaCO_3$) to represent a rock composition and a Polymethylmethacrylate – $(C_5O_2H_8)_n$ (PMMA) granular material to represent an organic mixture (a polymer powder). Four necessary EOS constants for each of the materials are summarised in Table 1. The material constants for the condensed constituents (the first phase of corresponding porous materials) are taken from literature and are in agreement with the well-known thermo-physical characteristics of the solid materials. The last two rows are the limiting initial density of the corresponding porous material ρ_b calculated

from Equation (16), below which the PTE Hugoniot is abnormal, and the corresponding critical porosity $m_b = \rho_{01}/\rho_b$. It should be noted that the limiting density, ρ_b, is slightly fluctuating with the change of porosity due to the mass concentration entering the formula in Equation (16) via the parameters c_{vs}, c_{vm}, etc. These thermo-mechanical parameters are constant only at a fixed mass concentration, i.e., for material with a given porosity. However, due to the large density mismatch between the condensed and gaseous phases this fluctuation typically affects only the third digit of the porosity value at the porosities up to m_b. The variation of ρ_b with porosity is noticeable only at extreme porosities above 100, when determination of the critical porosity m_b is not an issue because the Hugoniot behaviour is already abnormal at much lower porosities.

The majority of experimental Hugoniot data are taken from the popular compendiums [12-14] that summarize numerous experiments conducted in the world on the shock loading of condensed and porous materials.

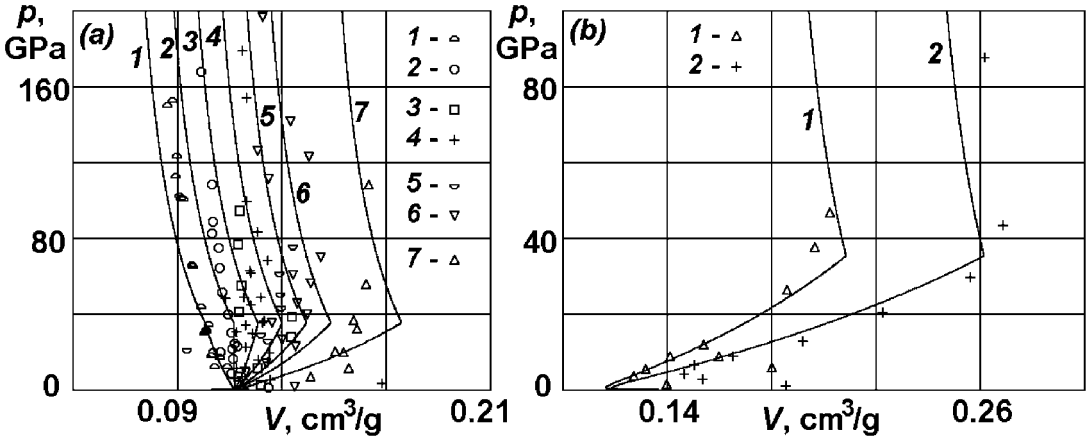

Figure 2 Calculated composite Hugoniots (curves) for copper powders compared with experiment (points) at different porosities (a): m = 1.4(1); 2.0(2); 2.5(3); 3.0(4); 3.5(5); 4.0(6); and 5.45(7), and (b): m = 7.2(1); and 10.034(2).

One of the most extensive sets of shock data obtained in the literature are the Hugoniots for copper at various porosities. A representative set of experimental points is drawn in Fig. 2 for pressures up to 2 Mbar and for 9 different porosities. It is seen that the critical Hugoniot indicating transition to the abnormality is curve 2 in Fig. 2(a) that corresponds to $m = 2$. This experimentally observed limiting porosity agrees very well with the calculated critical porosity $m_b = 2.02$ from Table 1. It is interesting to note that the Hugoniots visually originate from a single point. In fact, as it has been commented in the previous section regarding Fig. 1(c), the original point of the corresponding PTE Hugoniots is $v = v_f$. To illustrate, for the first three curves in Fig. 2(a), the actual originating points are v_f = 0.158(1); 0.224(2); and 0.28(3). That means that according to the analysis for the PTE Hugoniot in the present case $m_b = 2.02$ or $v_b = 0.2256$ and $v_f < v_b$ for curves 1 and 2, whereas $v_f > v_b$ for the remaining curves. Thus v_f may be far away from the visual point corresponding to $v = v_b$. The slight fluctuation of v_b is barely noticeable in Fig. 2(b) only at extreme porosities.

Commenting on observed deviations of calculated Hugoniots from the experimental points it is seen that they are greater for some selected porosities and vary from one porous material to another. For example, the observed error is within the experimental scatter for curves 5-7 at relatively high porosities but is moderate (about 8%) for curves 1 to 4. In particular, the accuracy of the Hugoniots at the extreme porosities shown in Fig. 2(b) is surprisingly good (less than 5%). It should be noted that accuracy in the primary compaction zone (within a few GPa for the loading pressure) is not expected to be good because of the kinetic processes involved in the compaction and strength of the material at these pressures (for detailed analysis, see [5, 6]). Nevertheless, even at low pressures the trend and behaviour of the PTE Hugoniot with a different observed p_c is correct. Several possible causes of the deviations at moderate porosities could be noted. The first one relates to experimental errors which will be discussed when analysing the next metallic powder. The second one could be a variation in experimental set-ups for different sets of data. For example, several points are taken from the compendium [13], and the majority from the collection [12] for the data set 2 in Fig. 1 for porosity m = 2. Finally, the compression behaviour is significantly affected by the cold part of an equation of state at moderate porosities when the behaviour of the condensed constituents predominates. This behaviour is obviously oversimplified with the use of the present EOS.

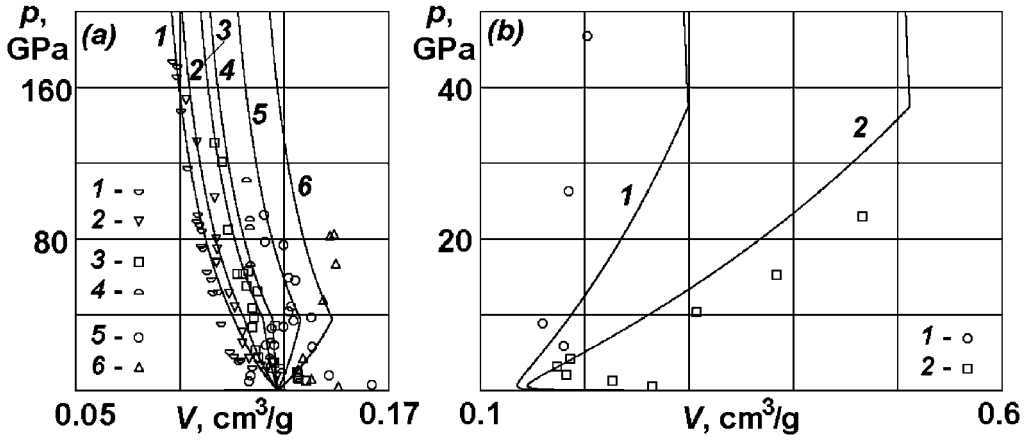

Figure 3 Calculated composite Hugoniots (curves) for iron powders compared with experiment (points) at different porosities (a): m = 1.129(1); 1.316(2); 1.653(3); 1.826(4); 2.328(5); and 2.9(6), and (b): m = 10.0(1); and 20.0(2).

The family of Hugoniots for a material with different condensed phase, iron, is summarised in Fig. 3. These results show similar scatter with some specifics related to selected porosities. In this case, the low-porosity description is even better than in the case of copper powders possibly due to a better description of the condensed phase by the present simple EOS. The transition to the abnormality is seen to occur between curve 4 and curve 5 that agree quite well with the experimental data (points 4 and 5). The corresponding porosities are 1.826 and 2.32 and the calculated critical porosity listed in Table 1 is m_b = 1.91. Thus, the agreement is again remarkably good. Data and calculations shown for high porosities in Fig. 3(b) look more divergent. For example, for porosity m = 10 (curve 1 and points 1), the error is close to 30%. However, it is well known and can be easily assessed from (1) that the density and specific volume errors for Hugoniots with the

shock and particle velocity errors $\Delta D/D$ and $\Delta u/u$, respectively, are of the order of $m(\rho/\rho_{01})(|\Delta D/D| + |\Delta u/u|)$. Thus, for a 1% error in experimental measurement of the Hugoniot particle and shock velocities, the density or specific volume error $\Delta v/v$ achieves as a minimum 10×0.02 (or 20%) for the m = 10 - porous material and it is proportionally larger at high compression with the factor of ρ/ρ_{01}. Correspondingly, for the m = 20 - porous material the error should be at least 40%. Keeping in mind that the Hugoniots are calculated with a constant Grüneisen parameters for different iron powders with the porosities from 1.129 up to 20 the description is actually very good. An interesting note can be made on the limiting volumes for the highly porous iron in Fig. 3(b). For porous materials with a moderate porosity the limiting specific volume is usually controlled by the PE Hugoniot such that $v_a < v_b$ with reference to the comment in the previous section. In the cases of Fig. 3(b) the limiting specific volume is controlled by the PTE Hugoniot ($v_b < v_a$) with $v_b \approx 0.243$ for the both porosities and $v_a \approx 0.258$ at m = 10 and $v_a \approx 0.47$ at m = 20. It is seen in Fig. 3(b) that the PTE Hugoniots at extreme porosities exhibit a noticeable variability of v_b.

The last set of metallic powders addressed in the report is analysed in Fig. 4. The description for Molybdenum powders is very good at porosities up to m = 4 and the last curve 4 in Fig. 4(a) can unfortunately be compared only for the experimental data available at pressures lower than the threshold value. Nevertheless, the error is quite moderate and disagreement of the calculated Hugoniots with the experimental points at the maximal pressure is approximately 18% which is not large for the porosity m = 8 following the error estimate discussed above. It should be reminded again that the low pressure behaviour is managed by kinetic mechanisms of the material deformation that are out of the scope of the present work. The Cobalt powder description shown in Fig. 4(b) and the Zinc powder description shown in Fig. 4(c) are very good for all available data that cover quite wide range of pressures both below and above the threshold pressure.

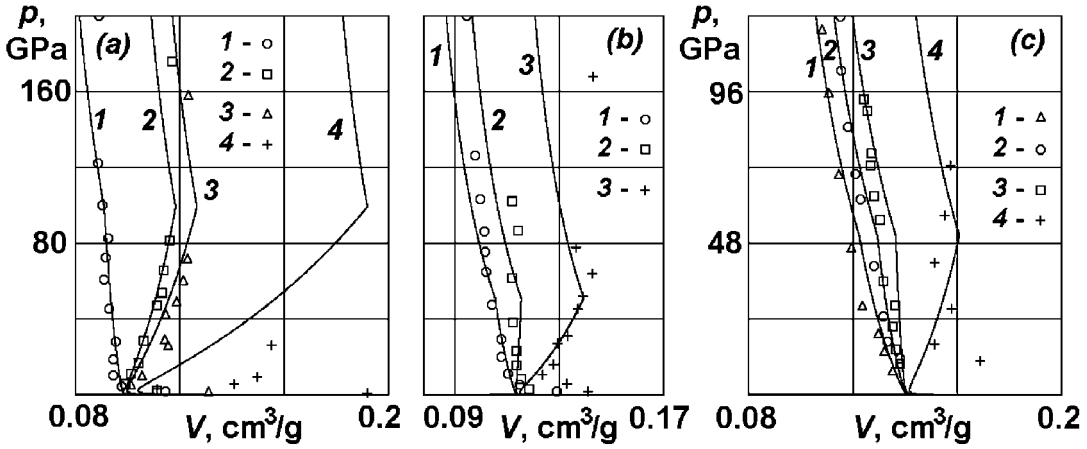

Figure 4 Calculated composite Hugoniots (curves) compared with experiment (points) for Molybdenum powders at different porosities (a): m = 1.82(1); 3.5(2); 4.0(3); and 8.0(4), for Cobalt powders (b): m = 1.59(1); 2.12(2); and 3.39(4), and for Zinc powders (c): m = 1.5(1); 1.798(2); 2.1(3); and 3.145(4).

The last was undertaken on organic and rock mixtures. The rock mixture represented by calcite porous materials is an interesting one and two experimental sets of data are analysed. The first dataset for low porosities (experimental points 1 in Fig. 5(a)) is taken from Ahrens *et al* [15] for porous Spergen limestone and the second dataset (points 2 and 3) are taken from the compendium by Trunin *et al* [12]. According to literature data, the Grüneisen parameter for calcite manifests some variability as noted below. The high-pressure data reported by Trunin *et al* [12] for calcite porous mixture have actually been borrowed from Kalashnikov *et al* [16]. This study determines the most suitable value for the Grüneisen parameter to be $\Gamma = 1.18$ that is used as a material constant in Table 1. However, a sharp increase of the parameter at pressures above 15 GPa from a value at normal conditions is discussed by Ahrens *et al* [15] possibly because of the calcite-aragonite transition at high temperatures and pressures [17] with claimed values below 1 at low pressure. This low-pressure value is not well defined and varies from 0.5 [17] to 0.98 in [18]. The nature of this two regime variation in Pasternak *et al* [18] is not explained but in view of the study by Kerley *et al* [17] it is likely to be associated with the phase transition. It is seen from Fig. 5(a) that these transition regimes are highly likely for this material and for many geological porous materials in general due to the abundance of silicone and calcite in rock compositions.

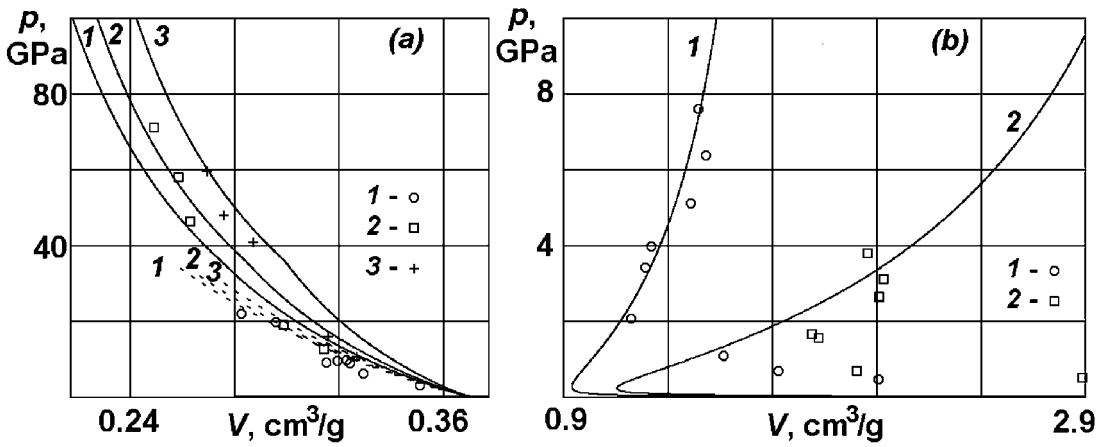

Figure 5 Calculated composite Hugoniots (curves) compared with experiment (points) for calcite powders at different porosities (a): m = 1.165(1); m = 1.319(2); and 1.563(3), and for PMMA powder (b): m = 10.782(1); and 23.72(2). Dashed composite Hugoniots for calcite 1-3 (a) are calculated with Γ = 0.5.

The data available for PMMA powders from Trunin *et al* [12] are used for the Hugoniot calculation shown in Fig. 5(b). The well-known assessment of the Grüneisen parameters at the reference conditions from bulk modulus, thermal expansion and heat capacity gives the value used in Table 1. The corresponding Hugoniots, assessed for these polymer powders and shown in Fig. 5(b), describe the experimental points very well within the experimentally available pressure region. The porosities are extreme, therefore, the variability of v_b is noticeable. It is interesting to note that because of a smaller density mismatch between the phases in this case the variability is essentially larger than for the iron powder in Fig. 3(b) at approximately the same porosity variation.

6. Conclusion

The work proposes a simple way of constructing reference Hugoniots for porous material using basic equations of state for the phases. These Hugoniots describe satisfactorily a variety of materials within a wide porosity range. This family of Hugoniots can be used for derivation of equations of state (EOSs) for a porous material with both normal and abnormal behaviour which could be useful for deriving EOSs in hydrocodes.

The Hugoniots designed are applicable within the 'hydrodynamic' pressure range, where the strength and material kinetic effects associated with the material packing and compaction are negligible. The non-hydrodynamic effects should be described by constitutive relations complementing the EOS. For advanced models, the inter-phase non-equilibrium or individual phase behaviour could be described directly either with an EOS integrating the non-equilibrium via some kinetic assumptions [4] or with constitutive relations dealing with the phase interaction [5-6, 11].

When the cold compression of a solid constituent exhibits elastically non-linear behaviour such as that substantially involving the Murnaghan EOS description, accuracy of the present description invoking simple EOS for the condensed phase can be worse at moderate porosities than at high porosities.

The inter-phase equilibration depends on the material microstructure which controls the time of equilibration. Therefore, some porous materials may demonstrate a better description with composite Hugoniots that extend transfer of the pressure-temperature equilibrium description above the pressure threshold, or the pressure equilibrium and temperature non-equilibrium description below the threshold.

7. References

1. Zeldovich Ya. B. and Raiser Yu. P., Physics of Shock Waves and High temperature Hydrodynamic Phenomena, Academic, New York, 1967.
2. Boshoff-Mostert L. and Viljoen H.J., Comparative study of analytical methods for Hugoniot curves of porous materials, J. Appl. Phys., 1999, v. 86(3), pp. 1245-1254.
3. Trunin R. F., Shock Compression of Condensed Materials, Cambridge University Press, 1998.
4. Fentona G., Grady D., and Vogler T.J., Modeling Thermodynamic Compression States In Distended Materials and Mixtures, Procedia Engineering, 2013, v. 58, pp. 724–731.
5. Resnyansky A.D., Constitutive Modelling of Hugoniot for a Highly Porous Material, J. Appl. Phys., 2008, v. 104 (9), pp. 093511-14.
6. Resnyansky A.D., Constitutive modeling of shock response of phase-transforming and porous materials with strength, J. Appl. Phys., 2010, v. 108 (8), pp. 083534-13.

7. Duffy J., Temperature Measurements during the Formation of Shear Bands in a Structural Steel, in: Mechanics of Material Behavior, G. Dvorak and R.T. Shield, Eds., Elsevier Science Pub., Amsterdam, 1984, p. 75.
8. Dorovskii V.N., Iskol'dskii A.M., and Romenskii E.I., Dynamics of impulsive metal heating by a current and electrical explosion of conductors, J. Appl. Mech. Tech. Phys., 1983, v. 24(4), pp. 454-467.
9. Godunov S.K., Kozin N.S., Romenskii E.I., Equations of state of the elastic energy of metals in the case of a nonspherical strain tensor, J. Appl. Mech. Techn. Phys., 1974, v. 15(2), pp 246-250.
10. Zharkov V.N. and Kalinin V.A., Equations of state for solids under high pressures and temperatures, N.Y.: Consultants Bureau, 1971.
11. Resnyansky A.D., Bourne N.K., Millett J.C.F., and Brown E.N., Constitutive modeling of shock response of polytetrafluoroethylene, J. Appl. Phys., 2011, v. 110(3), pp. 033530-15.
12. Trunin R.F., Gudarenko L.F., Zhernokletov M.V., Simakov G.V., Experimental data on shock wave compression and adiabatic expansion of condensed substances, [in Russian], Sarov, Russian Federal Nuclear Centre - VNIIEF, 2nd ed., 2006.
13. van Thiel M. (Ed.), Compendium of shock wave data, Livermore: Lawrence Livermore Laboratory Report UCRL-50108, 1977, pp. 142-148
14. Marsh S.P. (Ed.), LASL Shock Hugoniot Data, Univ. California Press, Berkeley, 1980.
15. Ahrens T.J. and Gregson V.G., Jr., Shock Compression of Crustal Rocks: Data for Quartz, Calcite, and Plagioclase Rocks, J. Geophys. Res., v. 69(22), 1964, pp. 4839-4874.
16. Kalashnikov N.G., Pavlovsky M.N., Simakov G.V., and Trunin R.F, Dynamic compressibility of calcite-group minerals, 1973, Izv. Earth Phys., n. 2, pp. 23-29.
17. Kerley G.I., Equations of state for calcite minerals. I. Theoretical model for dry calcium carbonate, High Pressure Research, 1989, v. 2(1), pp. 29-47.
18. Pasternak A., Lee E.L., and Miller D.G., Equation of state and shock entropy of $CaCO_3$, LLNL report UCID 17344, LLNL, Livermore, California, 1976.

DEFENCE SCIENCE AND TECHNOLOGY GROUP
DOCUMENT CONTROL DATA

1. DLM/CAVEAT (OF DOCUMENT)

2. TITLE

A Family of Reference Hugoniots for Two-phase Porous Materials

3. SECURITY CLASSIFICATION (FOR UNCLASSIFIED REPORTS THAT ARE LIMITED RELEASE USE (L) NEXT TO DOCUMENT CLASSIFICATION)

Document	(U)
Title	(U)
Abstract	(U)

4. AUTHOR(S)

A.D. Resnyansky

5. CORPORATE AUTHOR

Defence Science and Technology Group
PO Box 1500
Edinburgh South Australia 5111 Australia

6a. DST Group NUMBER	6b. AR NUMBER	6c. TYPE OF REPORT	7. DOCUMENT DATE
DST-Group-TR-3152	AR-016-394	Technical Report	June 2015

8. FILE NUMBER	9. TASK NUMBER	10. TASK SPONSOR	11. NO. OF PAGES	12. NO. OF REFERENCES
2015/1037961/1	CDF 07/403	VCDF	17	18

13. DST Group Publications Repository

http://dspace.dsto.defence.gov.au/dspace/

14. RELEASE AUTHORITY

Chief, Weapons and Combat Systems Division

15. SECONDARY RELEASE STATEMENT OF THIS DOCUMENT

Approved for public release

OVERSEAS ENQUIRIES OUTSIDE STATED LIMITATIONS SHOULD BE REFERRED THROUGH DOCUMENT EXCHANGE, PO BOX 1500, EDINBURGH, SA 5111

16. DELIBERATE ANNOUNCEMENT

No Limitations

17. CITATION IN OTHER DOCUMENTS Yes

18. RESEARCH LIBRARY THESAURUS

Hugoniot; Two-phase material; Porous material; Equation of state

19. ABSTRACT

Hugoniot states of heterogeneous materials obtained in shock experiments transit through various thermodynamic states that are not necessarily in equilibrium. Detailed numerical analysis employing a multi-phase constitutive material model has been conducted earlier which stressed the role of achieving equilibrium between the gaseous and condensed phases. The analysis also showed that the abnormal response of highly porous materials is closely associated with the attainment of the inter-phase equilibrium of both pressure and temperature. Mie-Grüneisen equations of state with the Murnaghan cold compression term were used earlier in the numerical analysis to illustrate the abnormal response. The present work shows that very simple equations of state for the phases are sufficient to describe the abnormality with the key necessary consideration a two-phase description of porous materials.